Stream Function-Vorticity flow in Lid-Driven Square Cavity: Computational and Visualization Analysis with Fine Mesh Grid

Santhana Krishnan Narayanan
PG and Research Department of Computer Science
Dr. Ambedkar Government Arts College
Chennai, Tamilnadu, India

Antony Alphonnse Ligori
Department of Mathematics
Gedu College of Business Studies
Royal University of Bhutan
Bhutan

Jagan Raj Soundarraj
Department of Chemistry
Vellammal Institute of Technology
Panchetti, Tamilnadu
India

Abstract:- A finite difference scheme is used with the Navier-Stokes equations for the completely coupled formulation of Stream Function-Vorticity. Fine Graded Mesh is used in the cavity to address vortex flow dynamics and gradual continuations for *Re=100, 1000, 8000 and 12,000* allows solutions to be computed in the grid of *32x32, 64x64, 128x128, 256x256, 512x512 and 1024x1024*. The formation of recent tertiary with quaternary corners vortex are visualized using advanced computer system in this work as a significant feature. Comparisons are done with standard queries in the given literatures and our results are found to be more accurate.

Keywords:- *Navier-Stokes Equation, Finite volume method, Discretization, Internal flow circulations, Corner eddies.*

I. INTRODUCTION

Lid-driven square cavity flow problems have witnessed a great deal of progress by recent researchers. By certain finite difference approaches, Navier-Strokes equations describes incompressible viscous fluids are overcome. Representation of incompressible viscous flows by Navier-Stokes equations are solved by many finite difference methods. Developments in computer technology hardware with 10th Generation intel$^{@}$core*i7 advanced computational algorithms have made it possible to make attempts towards core processor workstation computer system as well as in the study and numerical approach to highly complex flow problems.

High end processor workstation computer system as well as in the analysis and numerical solution of extremely complex flow problems, advanced numerical algorithms have allowed attempts to be made towards various lists such as Lid-driven square cavity. Harlow et al. [1] developed a new method for the limitation of which is partially constrained and slightly open numerical investigation of the time dependent flow of the incompressible fluid. Ghia et al. [2] investigated the two-dimensional Navier-Stokes vorticity-stream function formulation of an incompressible equations. Carlos et al. [3] solved the flow problem inside a square cavity, whose lid has constant pace. Zhang [4] found that multi-grid techniques are used to model the two-dimensional square-driven flow of cavities with small to large quantities of Reynolds numbers in compact fourth-order finite differential schemes. Erturk et al. [5] examined the 2-D steady incompressible driven cavity flow numerical calculations. Jun Zhang et al. [6] proposed an efficient Legendre-Gulerkin method of spectral elements for constant steady flows in rectangular cavities. Poochinapan [7] studied in the stream function formulation, the properties of approximations to nonlinear terms of the 2-D incompressible Navier-Stokes equations.

Barragy et al. [8] observed a new tertiary and quaternary corner vortex by a p-type finite element scheme. Sundarammal et al. [9-10] studied Graphical visualization for closed form solutions. The present study reflects an attempt to use the multigrid approach in the Navier-Stokes solution for a Lid-driven square cavity flow issue with an aim of achieving solutions as high as possible for Reynolds numbers and mesh refinements.

ISSN No:-2456-2165

II. MATHEMATICAL MODEL

The physical system known to have a two-dimensional steady state (2-D) length L of the lid-driven square cavity is shown in Figure 1. The flow inside a square cavity in which the top wall (lid) travels at a uniform level. Here, u and v are the ones that are parameters of the x and y directions of the velocity vectors, the fluid density and their constant viscosity μ.

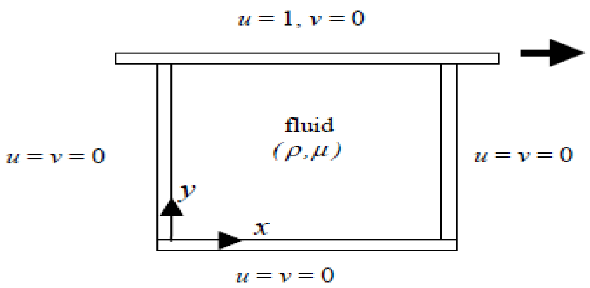

Fig. 1. Physical system of Lid-driven Square Cavity

The incompressible two dimensional Navier-Stokes equations with the lid velocity U_{Lid} , the mass and it is possible to write momentum equations in dimensionality form as

$$\frac{\partial u'}{\partial x'}+\frac{\partial v'}{\partial y'}=0$$

$$\rho\frac{\partial u'}{\partial t'}+\rho u'\frac{\partial u'}{\partial x'}+\rho v'\frac{\partial u'}{\partial y'}=-\frac{\partial p'}{\partial x'}+\left(\frac{\mu\partial^2 u'}{\partial x'^2}+\frac{\mu\partial^2 u'}{\partial y'^2}\right)$$

$$\rho\frac{\partial v'}{\partial t'}+\rho u'\frac{\partial v'}{\partial x'}+\rho v'\frac{\partial v'}{\partial y'}=-\frac{\partial p'}{\partial y'}+\left(\frac{\mu\partial^2 v'}{\partial x'^2}+\frac{\mu\partial^2 v'}{\partial y'^2}\right)$$

After non-dimensionalising, the mass and momentum equations can be written as

$$\frac{\partial u}{\partial x}+\frac{\partial v}{\partial y}=0$$

$$\frac{\partial u}{\partial t}+u\frac{\partial u}{\partial x}+v\frac{\partial u}{\partial y}=-\frac{\partial p}{\partial x}+\frac{1}{Re}\left(\frac{\partial^2 u}{\partial x^2}+\frac{\partial^2 u}{\partial y^2}\right)$$

$$\frac{\partial v}{\partial t}+u\frac{\partial v}{\partial x}+v\frac{\partial v}{\partial y}=-\frac{\partial p}{\partial y}+\frac{1}{Re}\left(\frac{\partial^2 v}{\partial x^2}+\frac{\partial^2 v}{\partial y^2}\right)$$

Here $u=\frac{u'}{U_{lid}}$, $v=\frac{v'}{U_{lid}}$, $x=\frac{x'}{L_{lid}}$, $y=\frac{y'}{L_{lid}}$,

$t=t'\frac{U_{lid}}{L_{lid}}$, $\rho=\frac{\rho'}{\rho_{ref}}$, $\mu=\frac{\mu'}{\mu_{ref}}$,

$p=\frac{p'-p_{ref}}{\rho U_{lid}^2}$ with *Re* being the Reynolds number,

$Re=\frac{\rho' U_{lid} L_{lid}}{\mu'}$ and

p is the pressure.

$$u=\frac{\partial\psi}{\partial x}, v=-\frac{\partial\psi}{\partial y}$$

$$\omega=\frac{\partial v}{\partial x}-\frac{\partial u}{\partial y}=-\left(\frac{\partial^2\psi}{\partial x^2}+\frac{\partial^2\psi}{\partial y^2}\right)$$

$$\frac{\partial\omega}{\partial t}+u\frac{\partial\omega}{\partial x}+v\frac{\partial\omega}{\partial y}=\frac{1}{Re}\left(\frac{\partial^2\omega}{\partial x^2}+\frac{\partial^2\omega}{\partial y^2}\right)$$

No slip boundary condition has been applied for *u* and *v* directions at bottom and side walls as

$$u=0 \text{ and } v=0$$

and in the top wall

$$u=U_{lid}=1 \text{ and } v=0$$

Here incompressible Navier-Stokes equations using the lid-driven cavity are solved with staggered grid for finite volume discretization. Pressure-Correction technique with 2-step time integration of Adams-Bashforth, ADI and Thomas algorithm is used to solve the poisson pressure equations. Second Ordered Central (SOC), the finite volume technique is fixed to discretize the governing functions and finite volume operator on the *x*-momentum and *y*-momentum equations are utilized to obtain the numerical solutions. Pre and Post processing is done using *Matlab* software.

III. RESULTS AND DISCUSSION

Set the fluid that is trapped inside a square cavity in motion by the upper wall, which is sliding towards from left to right at constant velocity. In figure 2, the domain is the square unit cavity [7] and the viscous incompressible flow is controlled by the equations of Navier-Stokes and powered by the upper wall. The viscous and pressure forces characteristics depend on the number of Reynolds, the broad clockwise-rotating hierarchy of eddies emerges, main whose position occurs near the geometric middle of the square cavity and many small eddies, secondary eddies rotating counter clockwise, tertiary eddies rotating clockwise whose locations occur at the three appropriate corners of the square. All the findings cited in this section were obtained using uniform Cartesian grids from the stream function-vorticity formulation version of a finite-difference variant.

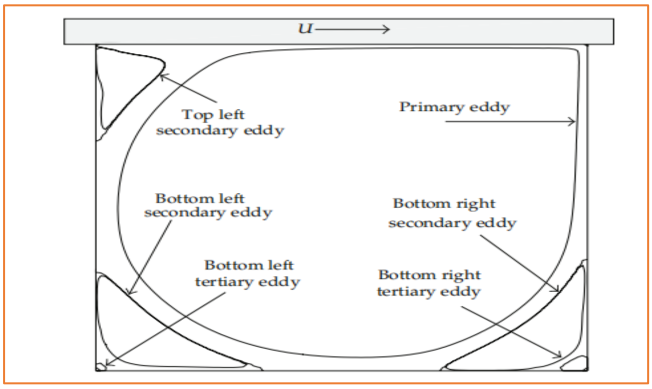

Fig. 2. Basic features of 2D flow circulation problem

The number of Reynolds, Re is the reflection of the fluid flow power, with the increase of Re the fluid flow becomes stronger. The flow domain is unchanged when the *Re* is increased. This greatly encourages analysis across the entire spectrum of the number of Reynolds, $0<Re<\infty$. Almost all phenomena that may occur in incompressible flows exhibit cavity flows such as primary eddies, corner eddies, corner singularities and secondary flows.

The top boundary velocity is set to be $u=1.0$ and $v=0$ for all five mesh grid of *32x32, 64x64, 128x128, 256x256, 512x512 and 1024x1024.* The grid is set to be *32x32* in figure 3-4. In Figure 3(a), in bottom corner right wall, single eddy is observed when *Re=100*. As Reynolds number increases to *1000* in the laminar flow, two eddies are observed in bottom corner of left and right boundary wall in figure 3(b). When Reynolds number moves from laminar flow to turbulent flow for *Re=8000*, three eddies are observed from two bottom corner walls and left top wall. It is observed that when *Re=100*, the starting to develop corner eddies in figure 3(a) and this growth being very rapid when *Re=1000* in figure 3(b). Note the growth of the eddy in the second corner in this process. When *Re=8000* in figure 3(c), the growth of corner eddy at the top wall is repeated indefinitely as the measure of Reynolds number rises. When *Re=12000*, the full growth of three corner eddies at all the walls are calculated and visualized in figure 3(d).

Figure 4 shows the stream function ψ patterns for four increasing Reynolds numbers, *Re=100, 1000, 8000 and 12000*. For *Re=100* in figure 4(a), the center of the primary eddy moves somewhat lower and to the right. When *Re=1000* in figure 4(b), the primary eddy centre moved lower and back to the centre plane. As *Re=8000* in figure 4(c), the center of the primary eddy to move toward the cavity's geometric centre. Further, as *Re=12000* in figure 4(d), the center of the primary eddy move below the geometric center. We observed as Re increases, the primary eddy centers moves through various positions.

The grid is set to be *64x64* in figure 5-6. In Figure 5(a), in bottom corner right wall, single eddy is observed when *Re=100*. As Reynolds number increases to *1000* in the laminar flow, two eddies are observed in bottom corner of left and right boundary wall in figure 5(b). When Reynolds number moves from laminar flow to turbulent flow for *Re=8000*, three eddies are observed from two bottom corner walls and left top wall. It is observed that when *Re=100*, the corner eddies begin to grow in figure 5(a) and this growth being very rapid when *Re=1000* in figure 5(b). Note the growth of the eddy in the second corner in this process. When *Re=8000* in figure 5(c), the growth of corner eddy at the top wall is repeated indefinitely as the amount of Reynolds number grows. When *Re=12000*, the full growth of three secondary corner eddies at all the walls and a bottom right tertiary eddy are calculated and visualized in figure 5(d).

Figure 6 shows the stream function ψ patterns for four increasing Reynolds numbers, *Re=100, 1000, 8000 and 12000*. For *Re=100* in figure 6(a), a little lower and to the right, the middle of the main eddy shifts. When *Re=1000* in figure 6(b), the main eddy core shifted lower and back to the centre plane. As *Re=8000* in figure 6(c), the center of the primary eddy heading toward the cavity's geometric centre. Further, as *Re=12000* in figure 6(d), the center of the primary eddy move below the geometric center. We observed as Re increases, the primary eddy centers moves through various positions.

The grid is set to be *128x128* in figure 7-8. In Figure 7(a), in bottom corner right wall, single eddy is observed when *Re=100*. As Reynolds number increases to *1000* in the laminar flow, two eddies are observed in bottom corner of left and right boundary wall in figure 7(b). When Reynolds number moves from laminar flow to turbulent flow for *Re=8000*, three eddies are observed from two bottom corner walls and left top wall. It is observed that when *Re=100*, the corner eddies are beginning to develop in figure 7(a) and this growth being very rapid when *Re=1000* in figure 7(b). Note the growth of the eddy in the second corner in this process. When *Re=8000* in figure 7(c), the growth of corner eddy at the top wall is repeated indefinitely as the number of Reynolds rises. When *Re=12000*, the full growth of three secondary corner eddies at all the walls and a bottom right tertiary eddy are calculated and visualized in figure 7(d).

Figure 8 shows the stream function ψ patterns for four increasing Reynolds numbers, *Re=100, 1000, 8000 and 12000*. In figure 8(a) for Re=100, the middle of the main eddy shifts a little lower and to the right. In Figure 8(b), as Re=1000, the centre of the main eddy shifted lower and back towards the centre plane. The middle of the main eddy shifts into the geometric centre of the cavity as Re=8000 in figure 8(c). Further, as *Re=12000* in figure 8(d), below the geometrical centre, the centre of the primary eddy shifts. We observed as Re increases, the primary eddy centers moves through various positions.

The grid is set to be *256x256*, 512x512 and 1024x1024 in figure 9-11 respectively. Figure 9-11 shows the stream function ψ patterns for four increasing Reynolds numbers, *Re=100, 1000, 8000 and 12000*. A little below and to the right, the middle of the main eddy moves for Re=100 in figure 9(a)-11(a). In Figure 9(b)-11(b), as Re=1000, the major eddy core moved lower and back toward the centre plane. As Re=8000 in Figure 9(c)-11(c), to travel into the geometric core of the cavity, the centre of the main eddy. Further, as *Re=12000* in figure 9(d)-11(d), the center of the primary eddy move below the geometric center. We observed as Re increases, the primary eddy centers moves through various positions. The comparison is made with Ghia et al [2] and found to be more accurate.

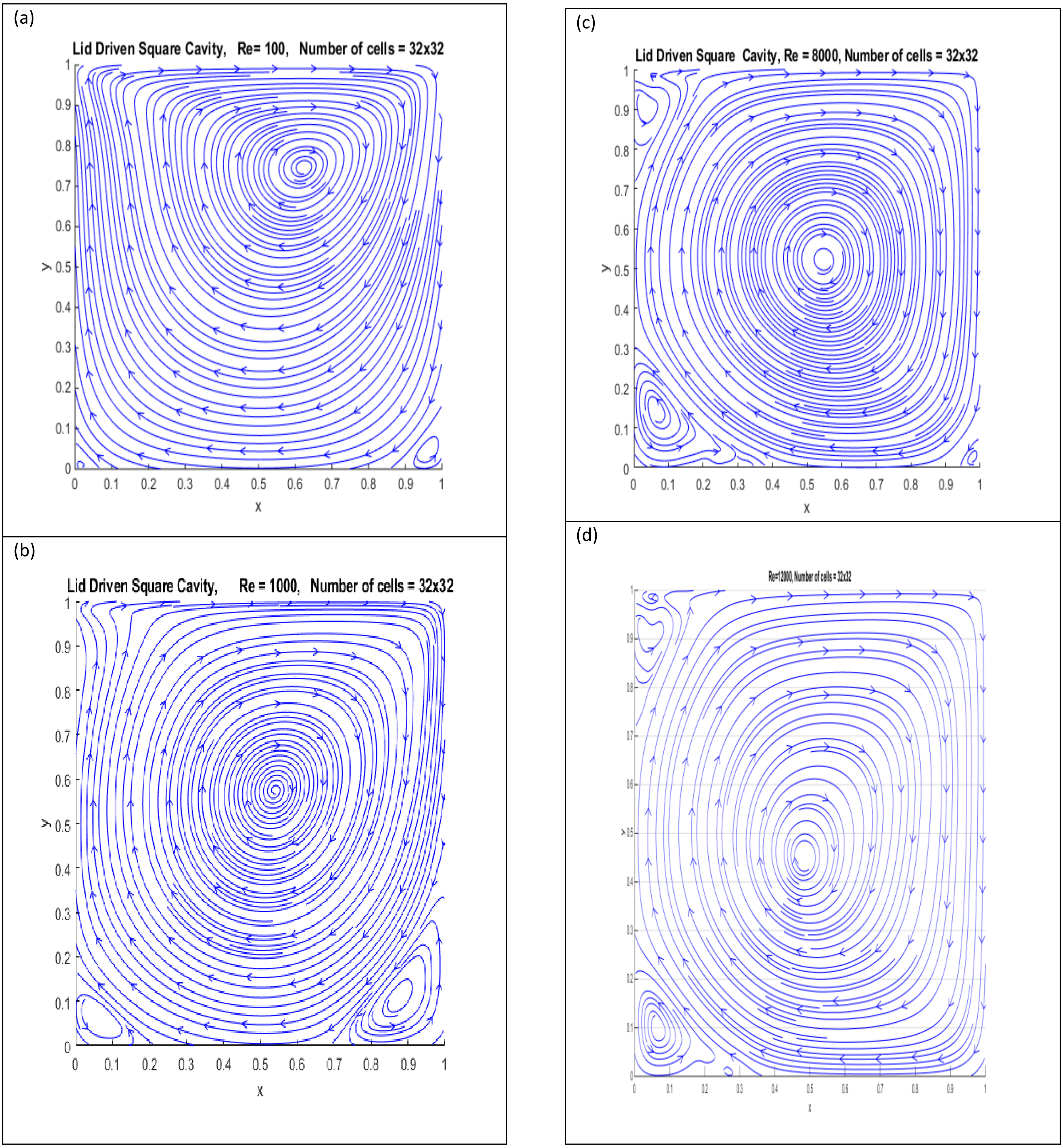

Fig. 3. Streamlines of the circulation of fluid in the square cavity for the ascending values of Reynolds Number with mesh *32x32* *(a) Re=100 (b) Re=1000 (c) Re=8000 and (d) Re=12000*

ISSN No:-2456-2165

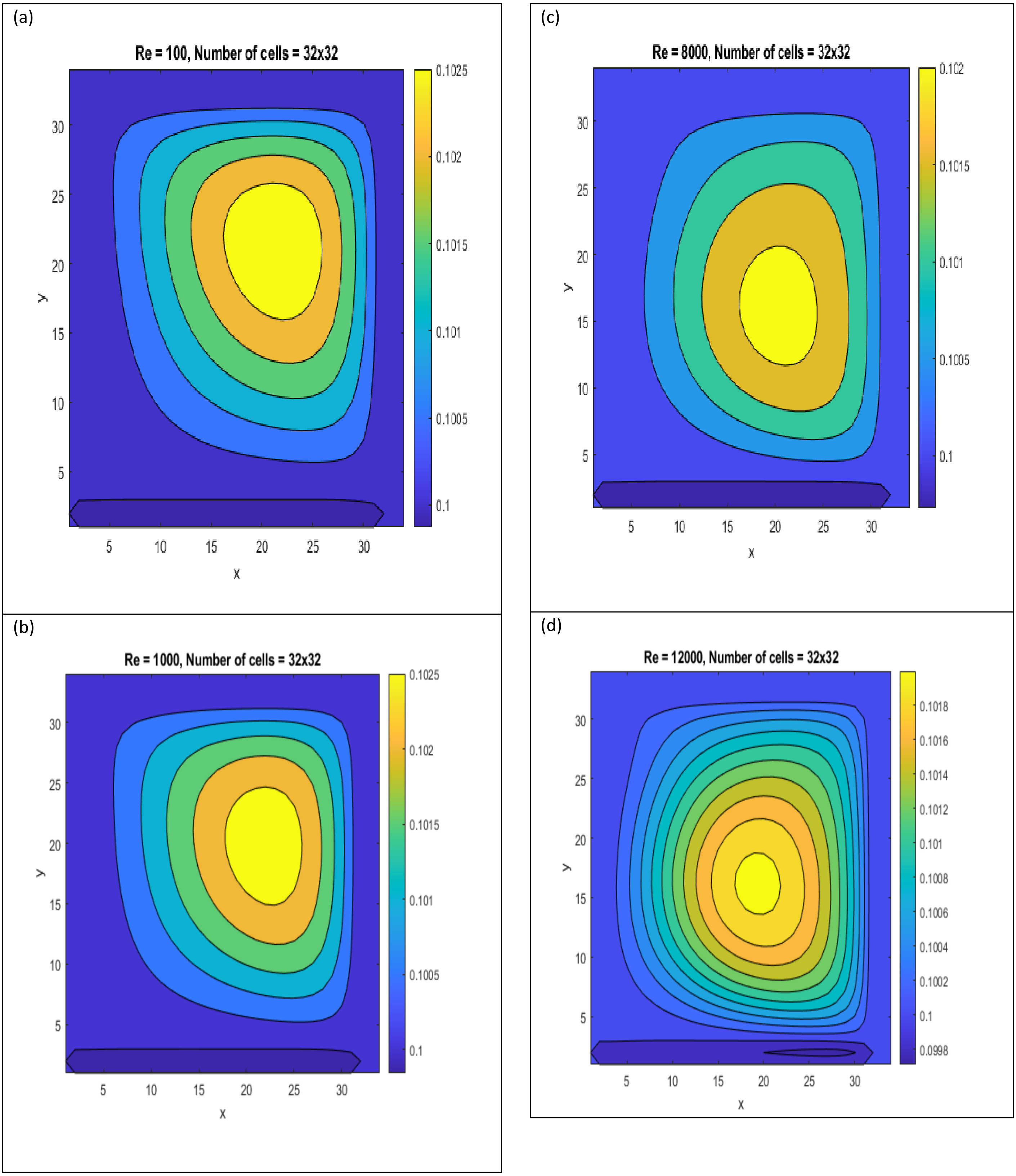

Fig. 4. Primary Eddy center of the Stream function moves towards the geometric center of the square cavity for the ascending values of Renolds Number with mesh *32x32* *(a) Re=100 (b) Re=1000 (c) Re=8000 and (d) Re=12000*

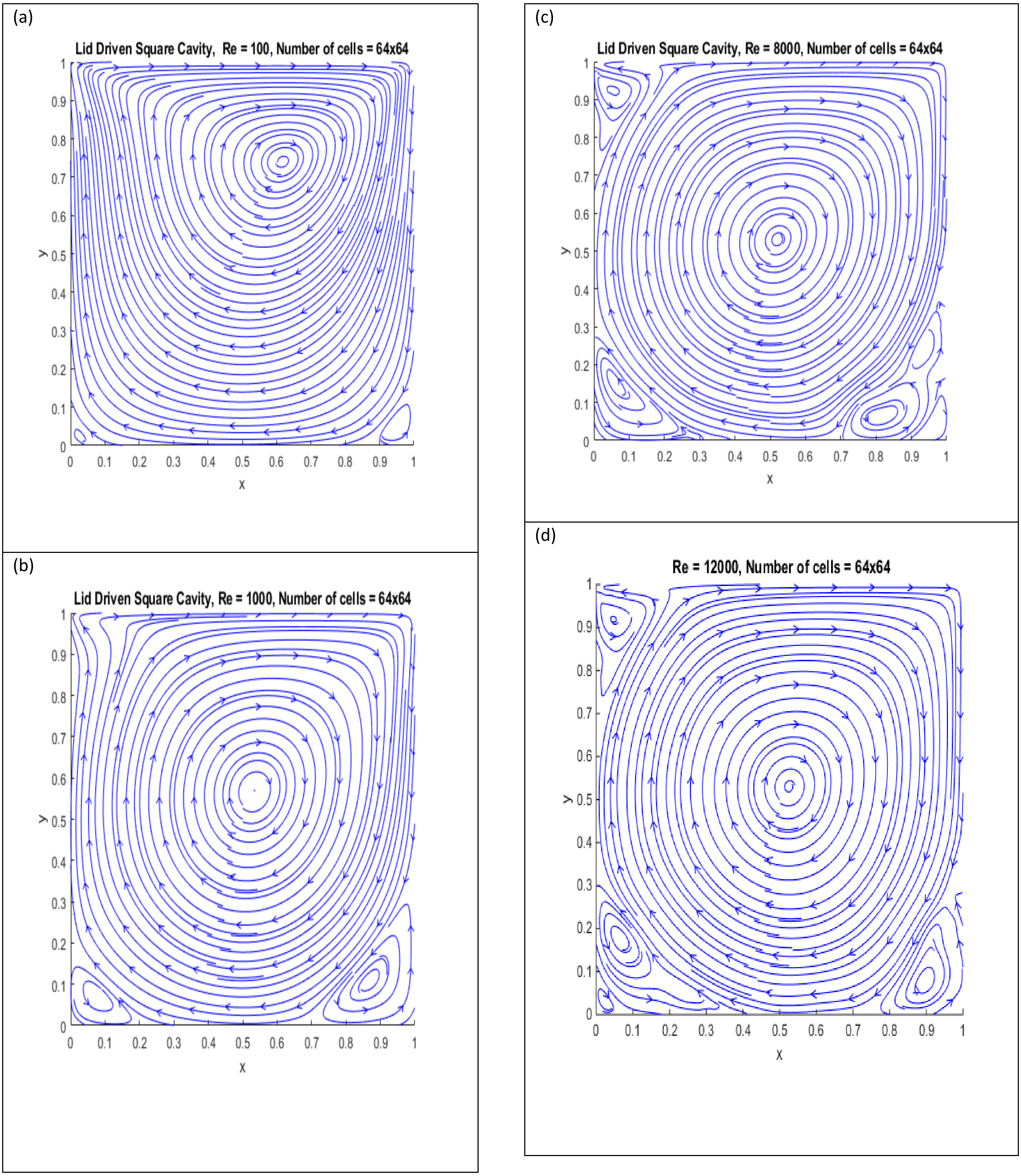

Fig. 5. Square cavity fluid flow streamlines for the ascending values of Reynolds Number with mesh 64x64(a) Re=100(b) Re=1000(c) Re=8000 and (d) Re=12000(a) Re=100(b) Re=1000(c) Re=8000 and (d) Re=12000

ISSN No:-2456-2165

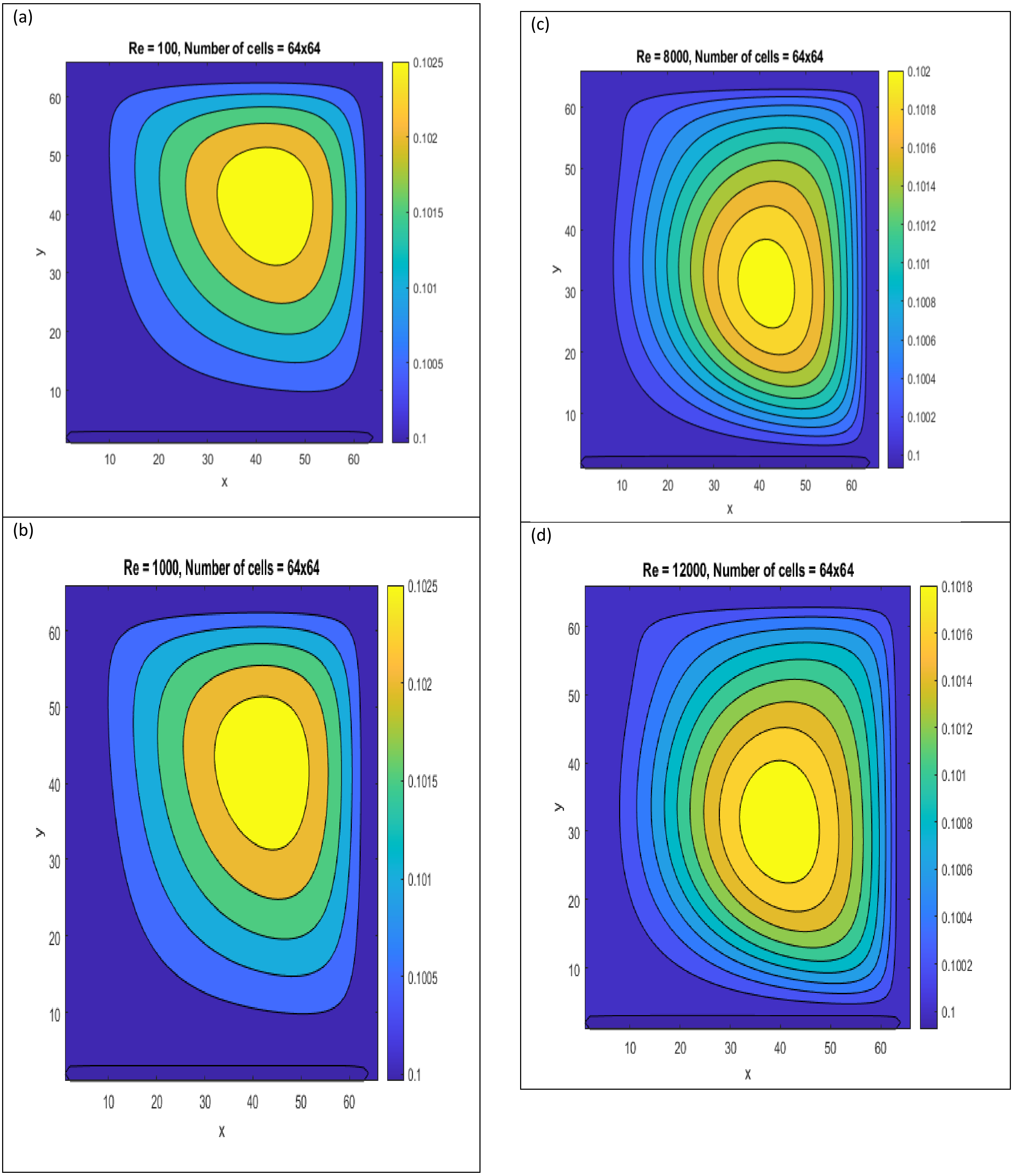

Fig. 6. For the ascending values of Reynolds Number with mesh 64x64 (a) Re=100 (b) Re=1000 (c) Re=8000 and (d) Re=12000, the main eddy centre of the stream function travels into the geometric center of the square cavity.

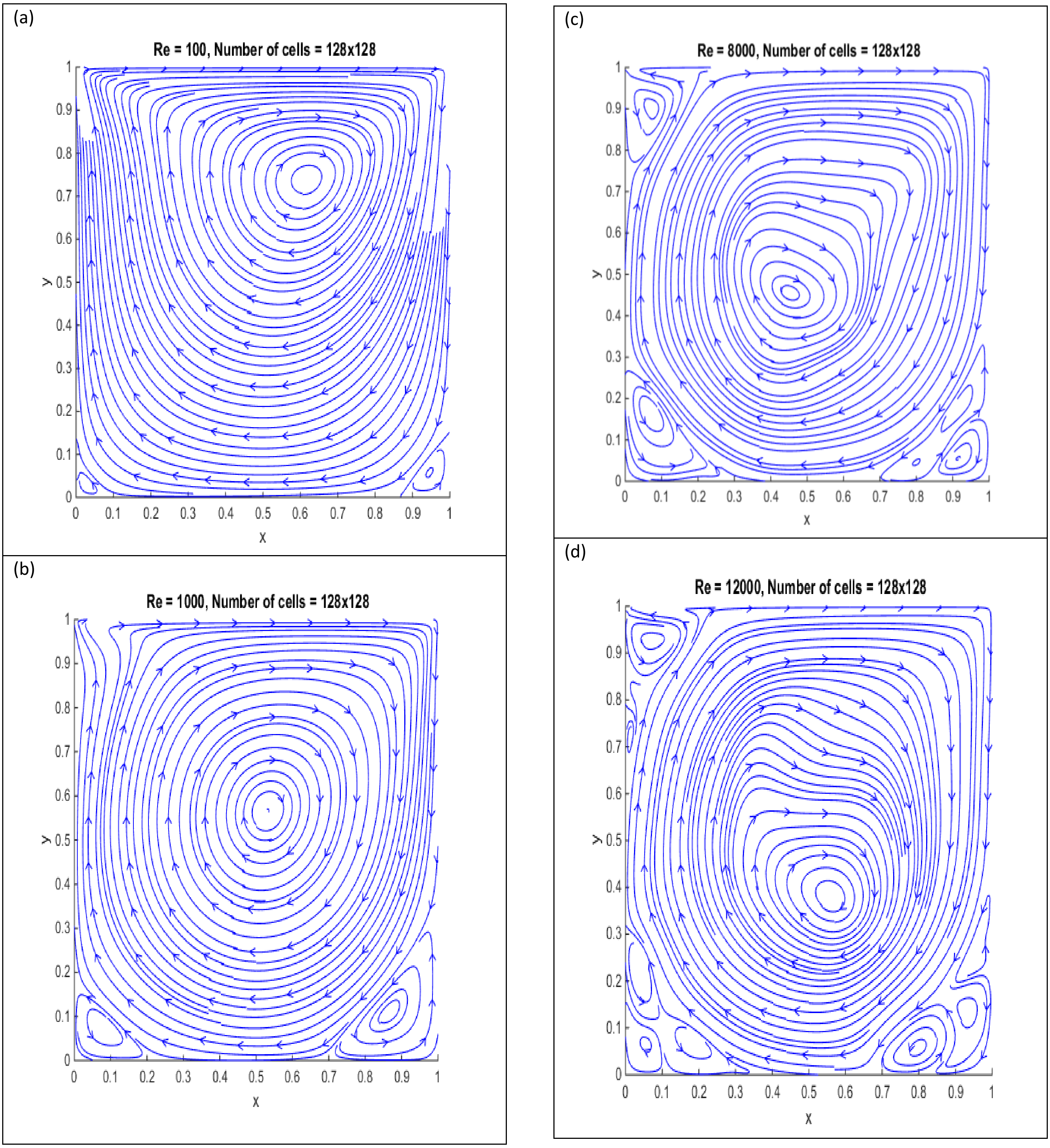

Fig. 7. Square cavity fluid flow streamlines for the ascending values of Reynolds Number with mesh 128x128(a) Re=100(b) Re=1000(c) Re=8000 and (d) Re=12000(b) Re=100(b) Re=1000(c) Re=8000 and (d) Re=12000

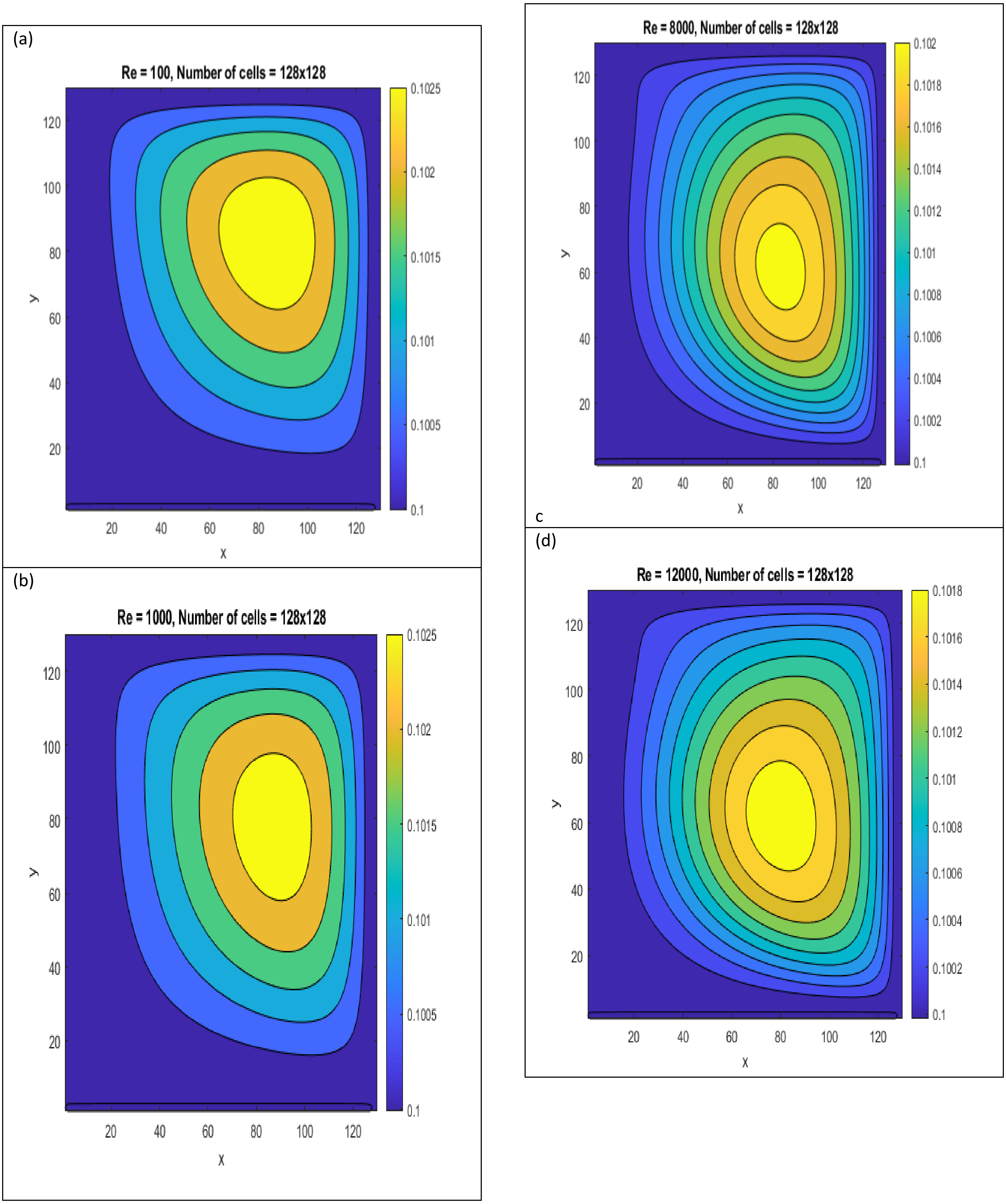

Fig. 8. For the ascending values of Reynolds Number with a mesh of 128x128 (a) Re=100 (b) Re=1000 (c) Re=8000 and (d) Re=12000, the main Eddy center of the Stream function travels into the square cavity's geometric centre.

ISSN No:-2456-2165

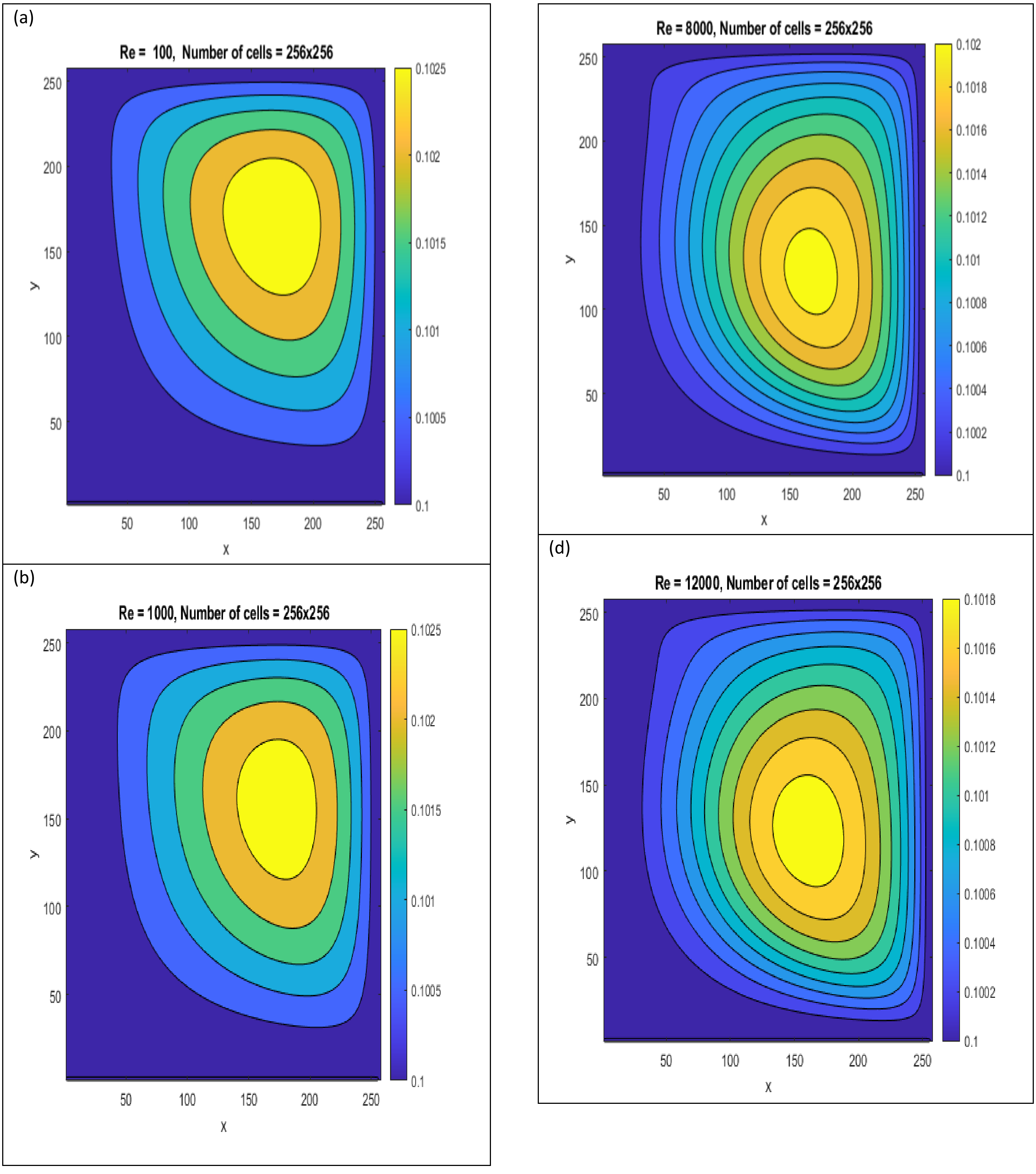

(c)

Fig. 9. The Eddy core of the Stream function moves to the geometric middle of the square cavity with mesh 512x512(a) Re=100(b) Re=1000(c) Re=8000 and (d) Re=12000(a) Re=100(b) Re=1000(c) Re=8000 and (d) Re=12000 for the ascending values of Reynolds Number with mesh 512x512,

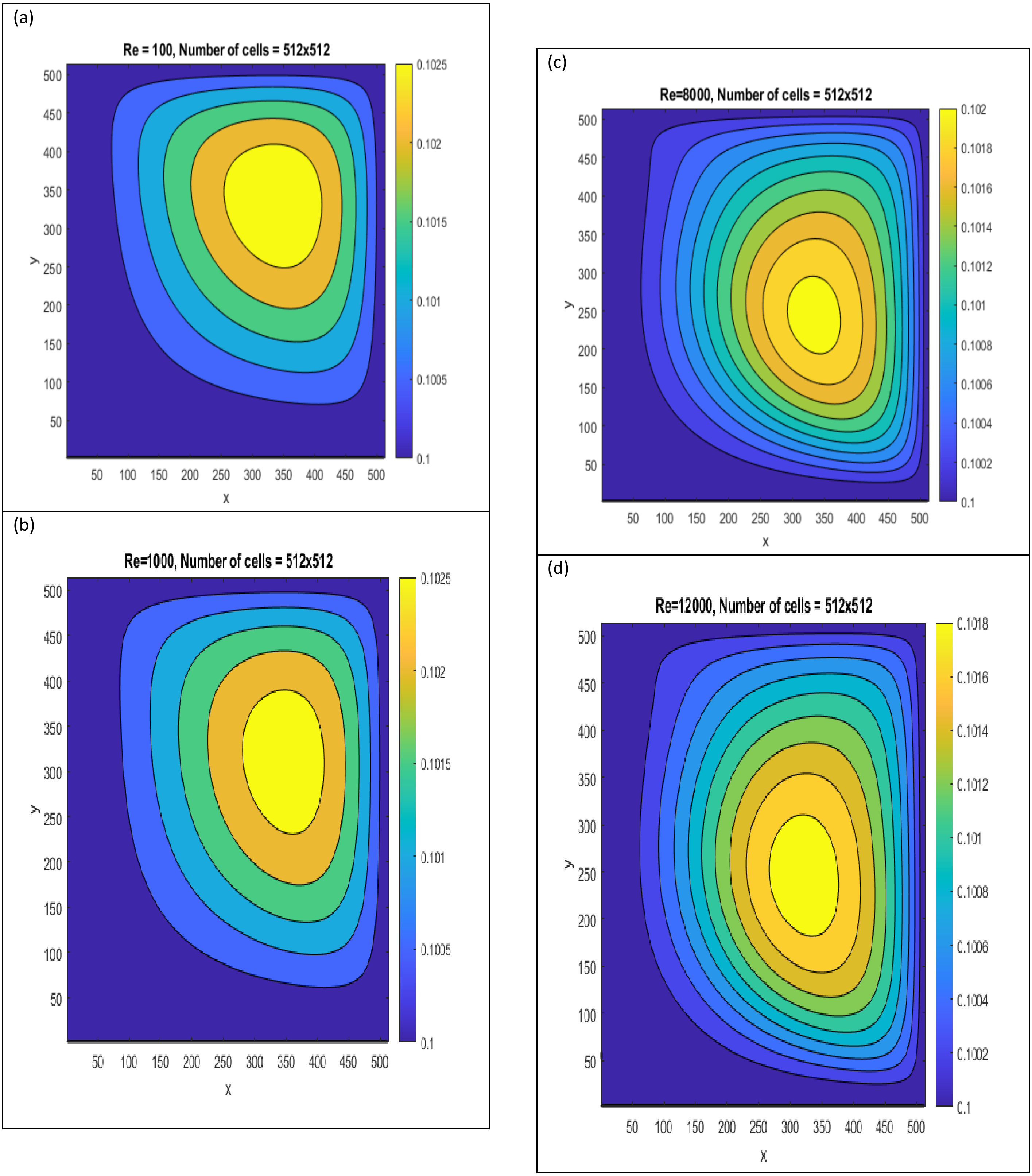

Fig. 10. For the ascending values of Reynolds Number with mesh 512x512, the main Eddy core of the Stream function travels into the geometric center of the square cavity with mesh 512x512 (a) Re=100 (b) Re=1000 (c) Re=8000 and (d) Re=12000

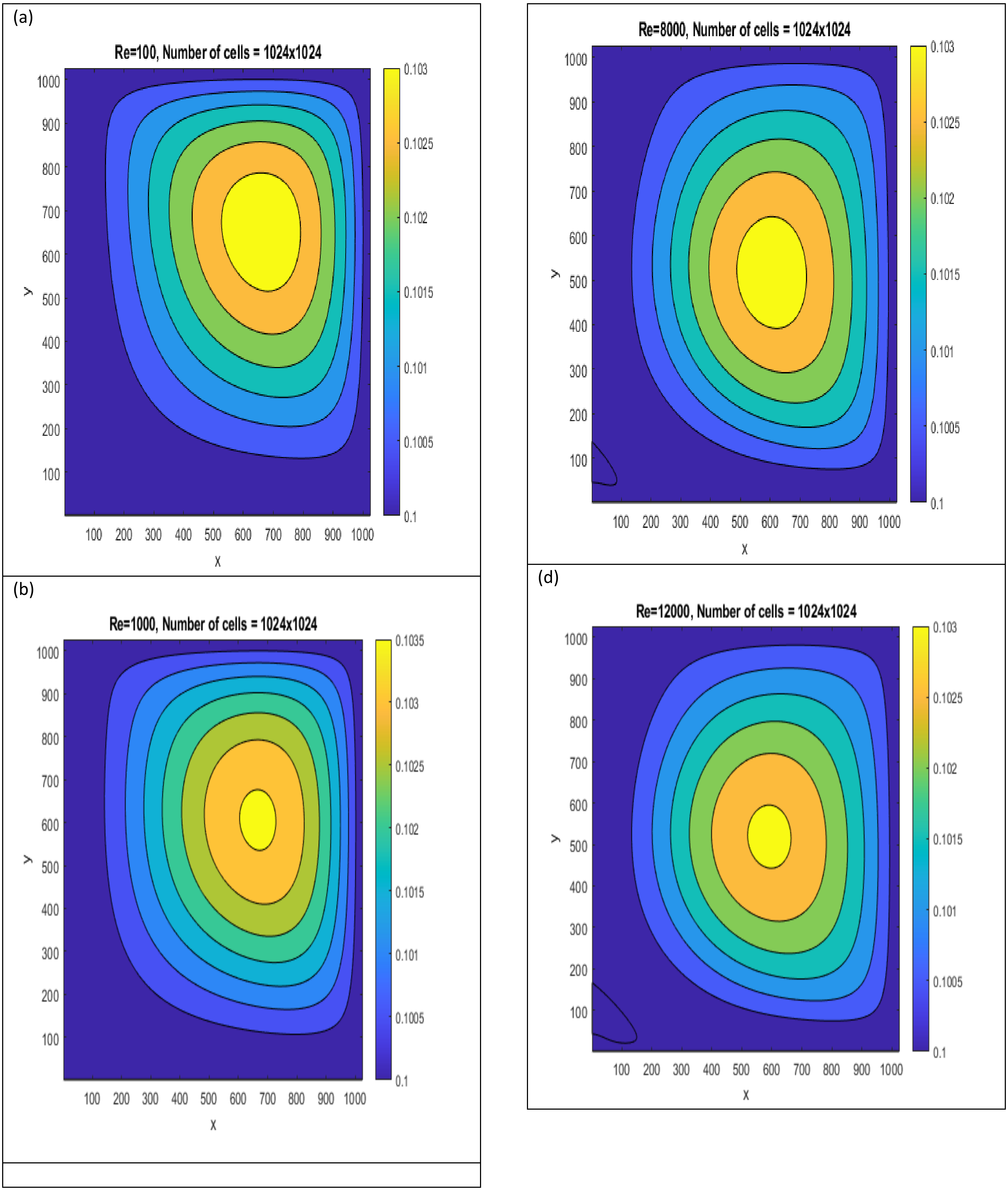

Fig. 11. For ascending values of Reynolds Number with mesh 1024x1024 (a) Re=100 (b) Re=1000 (c) Re=8000 and (d) Re=12000, the main Eddy core of the Stream feature travels into the square cavity's geometric centre.

IV. CONCLUSION

This paper extends previous work by Santhana Krishnan Narayanan et al.[11] to the Numerical solution visualization analysis with lid-driven square cavity flow of 32x32 and 64x64 mesh grid. For the laminar flow with *Re=100, 1000* and turbulent flow with *Re=8000, 12000* fine mesh solutions were obtained very efficiently. The finest mesh size used in the grid series, ***32x32, 64x64, 128x128, 256x256, 512x512 and 1024x1024***. A very critical parameter persists. The robustness and reliability of the overall solution strategies has been shown using this Lid-driven square cavity problem. Comprehensive specific outcomes have been presented. The present findings comply with published fine-grid solutions.

ACKNOWLEDGMENT

For their constructive suggestions, the writers acknowledge the suggestions and comments.

REFERENCES

[1]. Harlow F.H and Welch J.E, "Numerical Calculation of Time-Dependent viscous incompressible flow of fluid with free surface", The Physics of Fluids, Vol. 3, pp. 2182-2189, 1965.

[2]. Ghia V, Ghia K and Shin C, "*High resolutions for incompressible flow using the Navier-Stokes equations and a multigrid method*", Journal of computational Physics, Vol. 48, No. 3, pp. 387-411, 1982.

[3]. Carlos H.M, Roberta S and Araki L.K, "*The Lid-driven square cavity flow : Numerical solution with a 1024x1024 grid*", Journal of the Brazil Soc. of Mech. Sci. &Engg., Vol. XXXI, No. 3/191, pp. 186-198, 2009.

[4]. Zhang J, "Numerical simulation of 2D square driven cavity using fourth-order compact finite difference schemes, Computers and Mathematics with Applications, Vol. 45, pp. 43-52, 2003.

[5]. Erturk E, Carke T.C and Gokcol, "*Numerical solutions of steady incompressible driven cavity flow at high Reynolds number*", International Journal of Numerical methods in Fluids, Vol. 48, pp. 747-774, 2005.

[6]. Jun Zhang, Jianjun Jiao, Fubiao Lin, Wulan Li and Tao Sun, "*An efficient Legendre-Galerkin spectral element method for the steady flows in rectangular cavities*", Int. J. of Computer Mathematics, DOI: 10.1080/00207160.2019.1659962, Pp 1-14, 2019.

[7]. Poochinapan K, "Numerical Implementations for 2-D Lid-driven cavity flow in Stream function formulation", Int. Scholarly Research Network, Vol. 2012, pp 1-17, 2012.

[8]. Barragy E, Carey G.F, "*Stream Function-Vorticity driven cavity solution using p-finite element*", Computers and Fluid, Vol. 28, No. 5, pp. 453-468, 1997.

[9]. Sundarammal K., Ali. J. Chamkha and Santhana Krishnan Narayanan. "*MHD squeezes film characteristics between finite porous parallel rectangular plates with surface roughness*" International journal of Numerical methods for heat and fluid flow. Vol. 24(7): pp. 1595-1609, 2014.

[10]. Santhana Krishnan, Narayanan, Ali J. Chamkha and Sundarammal Kesavan., "*Squeeze film behavior in porous Transversely circular stepped plates with a couple stress fluid*", Engineering Computations, Emerald Publications, Vol. **33**(2), pp. 328–343, 2016.

[11]. Santhana Krishnan Narayanan, Antony Alphonnse Ligori and Jagan Raj, "*Visualization analysis of Numerical solution with 32x32 and 64x64 mesh grid lid-driven square cavity flow*", International journal of Innovative Science and Research Technology, Vol. 5, Issue 9, pp. 652-656, 2020.